ResearchGate

See discussions, stats, and author profiles for this publication at: https://www.researchgate.net/publication/257616024

Dielectric relaxations in PEEK by combined dynamic dielectric spectroscopy and thermally stimulated current

ARTICLE *in* JOURNAL OF THERMAL ANALYSIS AND CALORIMETRY · JANUARY 2013

Impact Factor: 2.04 · DOI: 10.1007/s10973-012-2548-3

CITATIONS
6

READS
20

4 AUTHORS, INCLUDING:

Eric Dantras
Paul Sabatier University - Toulouse III
79 PUBLICATIONS **465** CITATIONS
SEE PROFILE

Dandurand Jany
Paul Sabatier University - Toulouse III
64 PUBLICATIONS **399** CITATIONS
SEE PROFILE

C. Lacabanne
Paul Sabatier University - Toulouse III
338 PUBLICATIONS **3,607** CITATIONS
SEE PROFILE

Available from: Dandurand Jany
Retrieved on: 22 January 2016

J Therm Anal Calorim
DOI 10.1007/s10973-012-2548-3

Dielectric relaxations in PEEK by combined dynamic dielectric spectroscopy and thermally stimulated current

Aurélie Leonardi · Eric Dantras · Jany Dandurand · Colette Lacabanne

Received: 4 January 2012 / Accepted: 8 June 2012
© Akadémiai Kiadó, Budapest, Hungary 2012

Abstract The molecular dynamics of a quenched poly (ether ether ketone) (PEEK) was studied over a broad frequency range from 10^{-3} to 10^{6} Hz by combining dynamic dielectric spectroscopy (DDS) and thermo-stimulated current (TSC) analysis. The dielectric relaxation losses ε''_{KK} has been determined from the real part $\varepsilon'_{T(\omega)}$ thanks to Kramers–Kronig transform. In this way, conduction and relaxation processes can be analyzed independently. Two secondary dipolar relaxations, the γ and the β modes, corresponding to non-cooperative localized molecular mobility have been pointed out. The main α relaxation appeared close to the glass transition temperature as determined by DSC; it has been attributed to the delocalized cooperative mobility of the free amorphous phase. The relaxation times of dielectric relaxations determined with TSC at low frequency converge with relaxation times extracted from DDS at high frequency. This correlation emphasized continuity of mobility kinetics between vitreous and liquid state. The dielectric spectroscopy exhibits the α_c relaxation, near 443 K, which has been associated with the rigid amorphous phase confined by crystallites. This present experiment demonstrates coherence of the dynamics of the PEEK heterogeneous amorphous phase between glassy and liquid state and significantly improve the knowledge of molecular/dynamic structure relationships.

Keywords PEEK · Amorphous phase · Molecular mobility · Thermo-stimulated current · Dynamic dielectric spectroscopy

A. Leonardi · E. Dantras (✉) · J. Dandurand · C. Lacabanne
Physique des Polymères, Institut Carnot CIRIMAT, Université Paul Sabatier, 31062 Toulouse Cedex, France
e-mail: eric.dantras@univ-tlse3.fr

Introduction

Poly(ether ether ketone) (PEEK) has been synthesized in the 1980s and many works have been done to study its physical structure. The molecular structure of PEEK is presented in Fig. 1. Recently, a strong interest has been devoted to this polymer due to new issues as sizing, adhesion, or ageing [1]. The understood of structure/properties relationships is crucial.

For example, physical properties of thermostable thermoplastic polymers like PEEK are strongly dependent upon thermal history. These properties make PEEK an attractive high performance polymer for composite matrix and structural adhesive applications. PEEK can be obtained as quasi amorphous or semi crystalline film; it depends on the processing conditions from the molten state. The complexity of its amorphous phase was often studied by DSC [2–10]. PEEK is described with a 'three-phase model': crystallites, the mobile and the rigid amorphous fractions (RAF) [2–5], consistent with other low-crystallinity semiflexible polymers [11–13]. The RAF consist in 'amorphous' material highly constrained due to its proximity with crystalline phase. The temperature dependence of the amorphous phase molecular mobility has been already characterized by DMA [13–17], dielectric spectroscopy [4, 6, 18–20], and TSC [21–25]. Two subglass relaxations have been observed by dielectric spectroscopy and tentatively interpreted in terms of molecular motions. The γ relaxation is unaffected by variation in sample thermal histories [6]. The dynamic manifestation of the glass transition named α relaxation has been pointed out near 423 K. The temperature dependence of the α mode clearly exhibited a non-Arrhenius behaviour [19, 26]. A second peak, labelled α_c relaxation, at 468 K was due to relaxation of amorphous portion constrained by the crystal.

Published online: 18 July 2012

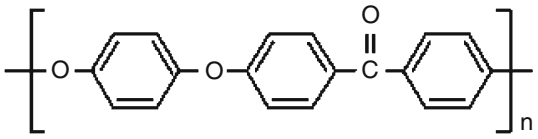

Fig. 1 Molecular structure of PEEK

Two components have been distinguished in the vicinity of the glass transition and associated with the molecular mobility of the 'true amorphous phase' and 'rigid amorphous region'.

The aim of this study is give rise to the relationships of the mobility kinetics in PEEK by combined liquid (dynamic dielectric spectroscopy) and vitreous (thermally stimulated currents) response and to shed some light on the complex dynamic above the glass transition temperature.

Experimental

Materials

The investigated PEEK samples were supplied by Victrex® (Aptiv™ 1000) in semi-crystalline sheets form of 100 μm. Thermal analyses were performed with a differential scanning calorimeter (Perkin-Elmer DSC 7) under nitrogen at a heating rate of 20 K^{-1} min to check the amorphous nature of PEEK. The samples ($\sim$10 mg) were placed in an aluminium pan and melted at 693 K for 15 min. Then there were quenched into liquid nitrogen in order to erase thermal history and to remove small nuclei that might act as seed crystals. Heating scans were recorded after quenching from the melt. Three DSC curves were performed in the same conditions.

Figure 2 shows the DSC curve of the quenched PEEK film. The heat capacity step at $T_g = 420$ K is associated with the glass transition characteristic of the amorphous phase. Upon heating, a sharp exothermic peak appears at $T_{cc} = 450$ K indicating a cold crystallization. A broad endothermic peak at $T_m = 610$ K is the melting. Thanks to the heat of melting for 100 % crystalline $\Delta H_\infty = 130$ J g^{-1} [7] the crystallinity ratio has been determined at $\chi_c = 6$ %. This low value of crystallinity for PEEK allows us to consider this sample as quasi amorphous.

The glass transition temperature of PEEK is $T_g = 427$ K. The number of entanglements in the amorphous zone of quenched sample is smaller, the chain mobility is increased and glass temperature appears at lower temperature [27].

The broad endothermic thermal manifestation is associated in the literature with a spherulitic morphology. Several authors [8–10] have suggested a dual morphology in which the thicker primary lamellae melts close to the equilibrium melting temperature and the thinner secondary lamellae melt at lower temperature, giving rise to the broad endotherm.

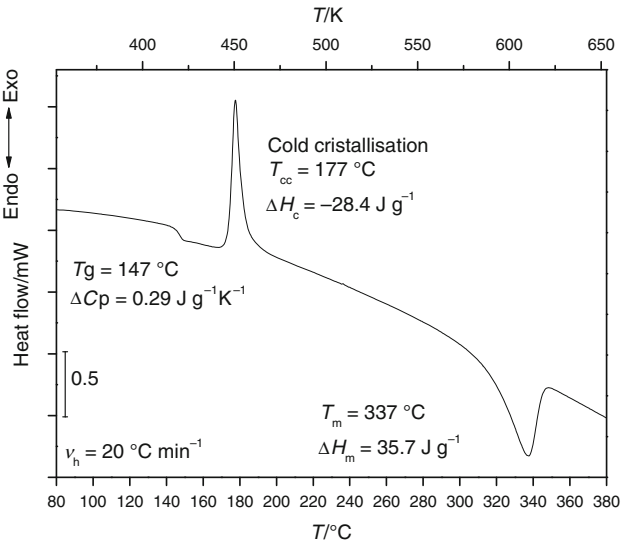

Fig. 2 Curve of quenched PEEK obtained by differential scanning calorimetry (DSC) from 353 to 653 K

Methods

Thermo-stimulated currents

TSC analyses were carried out on a TSC/RMA analyser developed in our laboratory and consisted of recording the depolarization current after removal a static field [28].

For recording complex thermogram, the sample was polarized by an electrostatic field $E_p = 6 \times 10^6$ V m^{-1} during $t_p = 2$ min over a temperature range from the polarization temperature T_p down to the freezing temperature T_0. T_p and T_0 were chosen according to the temperature range of the relaxation modes. Then the field was turned off and the depolarization current was recorded with a constant heating rate ($q_h = +7$ K min^{-1}), the equivalent frequency of the TSC thermograms was $f_{eq} \sim 10^{-2}$–10^{-3} Hz.

$$f_{eq} = \frac{1}{2\pi\tau(T_m)} \quad (1)$$

The equivalent frequency depend on the relaxation time $\tau(T_m)$ recorded at the temperature T_m at the maximum of elementary peak. Elementary TSC thermograms [29, 30] were recorded with a poling window of 5 K. Then the field was removed and the sample cooled down to a temperature T_p−40 K. The depolarization current was recorded with a constant heating rate q_h. The series of elementary thermograms was recorded by shifting the poling window by 5 K towards higher temperature.

The relaxation times, obtained by fractional polarisation (FP), of all elementary thermograms obey the Arrhenius equation:

$$\tau_{(T)} = \tau_{\mathrm{oa}} \cdot \exp\left(\frac{\Delta H}{RT}\right) \tag{2}$$

where τ_{oa} is the pre-exponential factor, ΔH the activation enthalpy, R the gas constant, and

$$\tau_{\mathrm{oa}} = \frac{h}{k_{\mathrm{B}}T}\exp\left(\frac{-\Delta S}{R}\right) \tag{3}$$

where h is the Planck constant, k_{B} is the Boltzmann constant, and ΔS the activation entropy.

Activation enthalpies of non-cooperative process follow the Starkweather's 'line' corresponding to the theoretical activation enthalpy ΔH_0 associated with zero activation entropy. It obeys the following law [31]:

$$\Delta H_{\Delta S=0} = RT\left(\ln\frac{k_{\mathrm{B}}T}{2\pi h f_{\mathrm{eq}}}\right) \tag{4}$$

According to William–Hoffmann–Passaglia model, cooperative movements depend to the length of mobile sequences and the relaxation times of processes isolated from FP obey a compensation law:

$$\tau_{(T)} = \tau_{\mathrm{c}} \cdot \exp\left[\frac{\Delta H}{R}\left(\frac{1}{T} - \frac{1}{T_{\mathrm{c}}}\right)\right] \tag{5}$$

The compensation law assumes that all entities relax at the compensation temperature T_{c} with the relaxation time τ_{c}.

Dynamic dielectric spectroscopy

Broadband dielectric measurements (DDS) were performed using a Novocontrol spectrometer covering a frequency range of 10^{-2}–10^{6} Hz. This technique has been extensively described by Kremer and Schönhals [32]. The frequency scans were carried out isothermally following a temperature step of 5 K between 123 and 523 K. The complex dielectric permittivity $\varepsilon^*_{T(\omega)}$ was recorded. Relaxation modes were fitted with the Havriliak–Negami equation [33]:

$$\varepsilon^*_{T(\omega)} = \varepsilon_\infty + \frac{\varepsilon_S - \varepsilon_\infty}{\left(1 + (i\omega\tau_{\mathrm{HN}})^{\alpha_{\mathrm{HN}}}\right)^{\beta_{\mathrm{HN}}}} \tag{6}$$

where ε_∞ is the relative real permittivity at infinite frequency, ε_{s} is the relative real permittivity at zero frequency, τ_{HN} is the relaxation time, α_{HN} and β_{HN} are the Havriliak–Negami parameters and ω is the angular frequency.

Dipolar relaxations are often hidden by dissipative losses due to ohmic conduction. The Kramers–Kronig transform [34] offer an analytical tool for calculate $\varepsilon''_{\mathrm{KK}}$ from the real part $\varepsilon'_{T(\omega)}$:

$$\varepsilon''_{\mathrm{KK}(\omega_0)} = \left(\frac{\sigma_0}{\varepsilon_0\omega_0}\right) + \frac{2}{\pi}\int_0^\infty \varepsilon'_{(\omega)}\frac{\omega_0}{\omega^2 - \omega_0^2}\cdot d\omega \tag{7}$$

Since the conductivity hindered observing high-temperature phenomena, some authors [5, 35] used complex modulus formalism to extract the Havriliak–Negami relaxation times τ_{HN}, instead of Kramers–Kronig equation.

$$M^*_{\mathrm{HN}(\omega)} = M_\infty + \frac{M_{\mathrm{S}} - M_\infty}{\left(1 + \left(\frac{-i}{\omega\tau_{\mathrm{HN-M}}}\right)^{\alpha_{\mathrm{HN}}}\right)^{\beta_{\mathrm{HN}}}} \tag{8}$$

The dynamic of the liquid state is explored thanks to these previous formalisms and gives access to relaxation times of the primary relaxation. The relaxation times of α primary relaxation are generally not linear in an Arrhenius diagram. They can be described by a Vogel–Tamman–Fulcher (VTF) equation [32]:

$$\tau_{(T)} = \tau_{0\mathrm{v}} \cdot \exp\left(\frac{1}{\alpha_{\mathrm{f}}(T - T_\infty)}\right) \tag{9}$$

where $\tau_{0\mathrm{v}}$ is the pre-exponential factor, α_{f} is the thermal expansion coefficient of the free volume, and T_∞ is the critical temperature at which any mobility is frozen.

Results

The quasi amorphous samples 100 μm thick were prepared by melting the as-received PEEK at 693 K for 15 min, directly on aluminium electrodes (1 cm diameter). The complex TSC thermograms and its fine structure show three dipolar modes on all the studied temperature range.

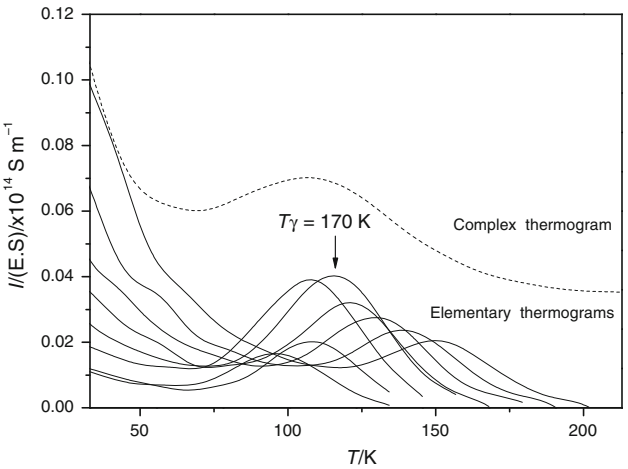

Fig. 3 Complex thermogram (*dot dash*) with $T_{\mathrm{p}} = 293$ K and elementary thermograms of the γ relaxation isolated by FP procedure with a polarisation window $\Delta T = 5$ K, T_{p} varies from 98 to 208 K

The γ mode shown in Fig. 3 appeared at 170 K. A secondary relaxation mode at 163 K with a shoulder at 198 K were previously reported in TSC experiments of PEEK with $\chi_c = 10$ % [23]. The difference between the two crystallinity ratios does not explain the modification of the TSC response. The dissimilarity of the results is explained by the fact that PEEK suppliers have changed the processing conditions. At low temperature, interfacial polarisation appears and is due to stress relaxation at the interface between free and rigid amorphous phase. A supplementary relaxation mode labelled β was observed at 343 K in Fig. 4. A primary relaxation mode named α was showed in Fig. 5. As the temperature of the α peak is in agreement with the glass transition temperature determined by differential scanning calorimetry, it has been associated with the dielectric manifestation of glass transition. This primary relaxation was more intense than secondary relaxation modes and a linear relationship between the applied field E_p and the magnitude of each peak is observed. It is characteristic of a dipolar depolarisation.

The ε'' evolution has been measured with DDS in the temperature range from 123 to 523 K between 10^{-2} and 10^6 Hz. The corresponding dielectric surface is presented in Fig. 6 and give rise to the appearance of two secondary relaxations γ and β then the α primary relaxation. Samples were prepared with the thermal treatment previously described.

The relaxation times extracted from M'' and the Kramers–Kronig transform applied to ε'' data were compiled on the same Arrhenius diagram in Fig. 7. We point out γ, α, and α_c. We focused on Kramers–Kronig transform due to the effective relaxation mode fitting of the α main relaxation. The relaxation loss ε''_{KK} deduced from $\varepsilon'_{T(\omega)}$ and corresponding to the α_c relaxation mode is showed in Fig. 8. These results have shown the fruitful synergy of TSC/DDS combination. In the case of β mode only an

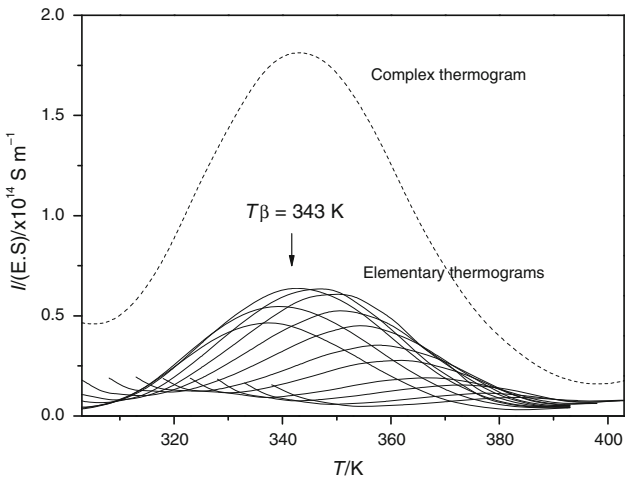

Fig. 4 Complex thermogram (*dot dash*) with $T_p = 413$ K and elementary thermograms of the β relaxation isolated by FP procedure with a polarisation window $\Delta T = 5$ K, T_p varies from 278 to 413 K

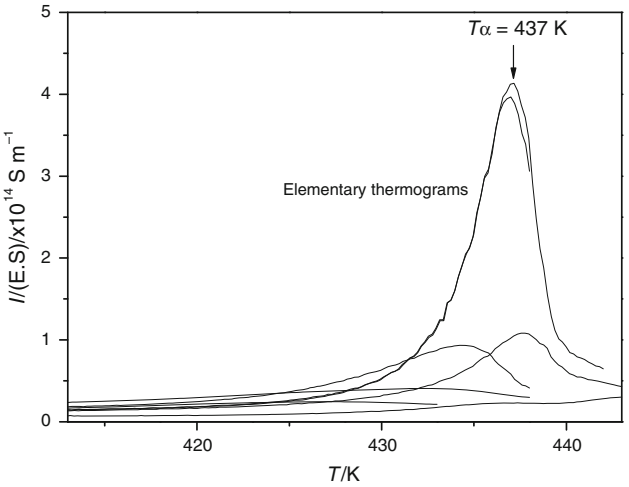

Fig. 5 Elementary thermograms of the α relaxation isolated by FP procedure with a polarisation window $\Delta T = 5$ K, T_p varies from 363 to 443 K

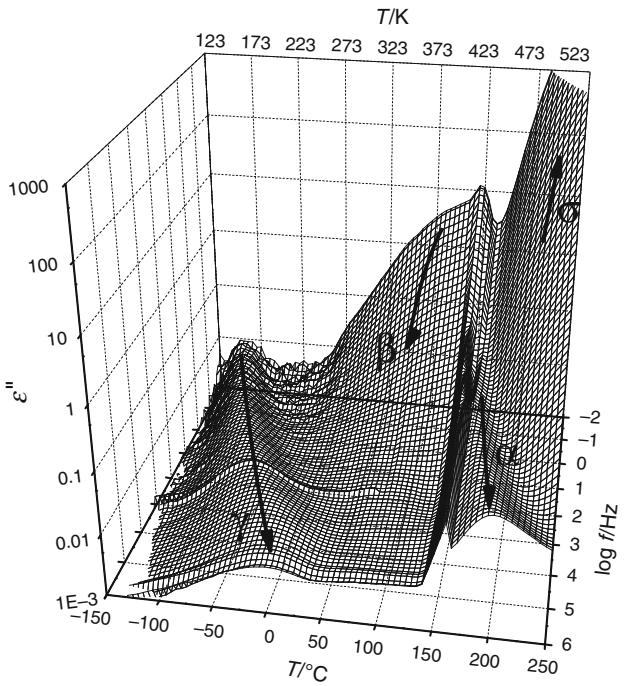

Fig. 6 Dielectric surface of ε'' PEEK in the temperature range from 123 to 523 K between 10^{-2} and 10^6 Hz

increase of dielectric loss at low frequency is observed and prevented us for a precise extraction of relaxation times.

Discussion

Liquid response

Activation enthalpies of isolated processes was extracted from FP procedure and presented in Fig. 9. Activation

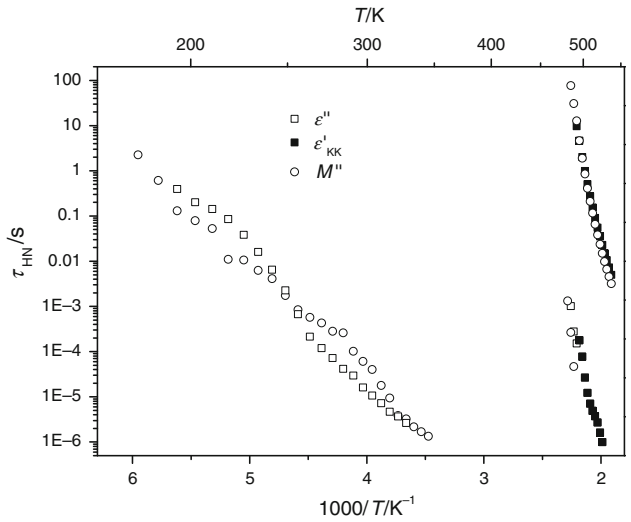

Fig. 7 Comparison on an Arrhenius diagram of relaxation times extracted by DDS permittivity (*open square*) and modulus (*open circle*) formalisms then by Kramers–Kronig transform (*filled square*)

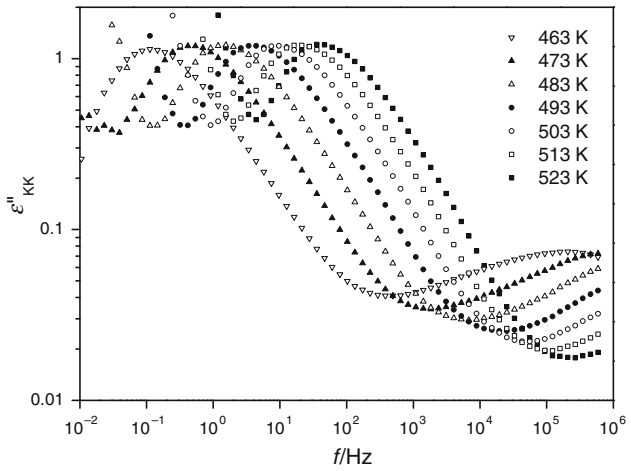

Fig. 8 The calculated relaxation loss ε''_{KK} corresponding to the α_c relaxation mode, deduced from $\varepsilon'_{T(\omega)}$, as a function of frequency, between 463 and 523 K

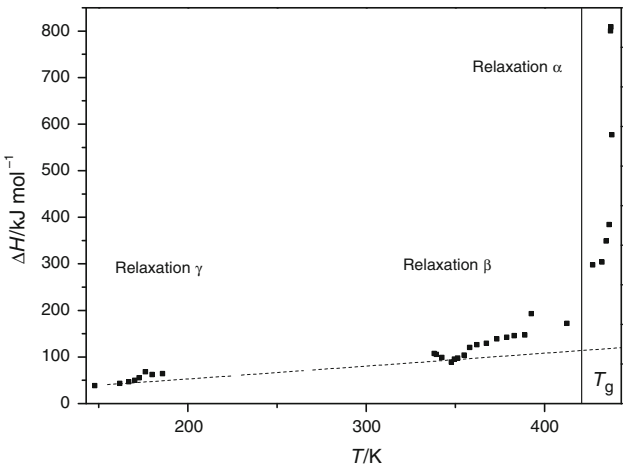

Fig. 9 Temperature dependence of the activation enthalpy determined from analysis of elementary FP TSC peaks. The *dash line* corresponds to Starweather's 'line'. The *straight line* represents the thermodynamic glass transition temperature

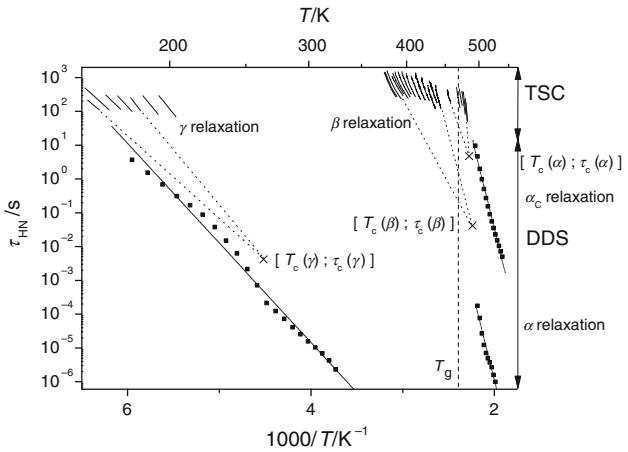

Fig. 10 Comparison on an Arrhenius diagram of relaxation times extracted by TSC elementary thermograms (*solid line*) and DDS results (*symbols*, *dotted lines* are a guide for the eyes). The *vertical dashed line* represents thermodynamic glass transition temperature. The *dotted lines* represent extrapolations that give rise to the compensation point ($[T_c\ (\gamma) = 221$ K; $\tau_c\ (\gamma) = 4 \times 10^{-3}$ s] $[T_c\ (\beta) = 447$ K; $\tau_c\ (\beta) = 4 \times 10^{-2}$ s] $[T_c\ (\alpha) = 440$ K; $\tau_c\ (\alpha) = 5$ s])

enthalpies of γ and β secondary relaxations followed the Starkweather line; they have been associated with non-cooperative mobility of localized dipoles. According to the Eq. (3) of τ_{0a}, when entropy is null, the pre-exponential factor is closed to 10^{-12} s. This time is enough slow to permit reorientation of localised entities. For the main α relaxation the values ΔH depart from this line, it has been attributed to delocalized molecular mobility of cooperative motions. Non cooperative versus cooperative behaviour would be essentially controlled by the length of mobile sequences involved in a given processes. The temperature dependence of the relaxation times has been plotted in Fig. 10. Possible molecular origins of these relaxations are suggested [14, 36] more particularly by ^{13}C NMR [37]. A compensation temperature $T_c\ (\gamma)$ concerning γ mode appeared at low temperature. This localized mobility might be attributed to the rotational mobility of phenylene rings, the ether–ether rings were found to be more mobile than the ether–ketone rings [18–20]. Accordingly, the structure of amorphous polymers is described as a regular packing of repeats units in which there are some disorders sites. The molecular displacements are supposed to be initiated in these sites [16]. Relaxations time corresponding to molecular motions involved in the β relaxation converge in $T_c\ (\beta)$ close to the cold crystallisation temperature T_{cc}. This phenomenon was attributed to inter macromolecular localized conformational defects displacement. At

crystallisation temperature T_{cc}, conformational defects reorganised due to the increase of crystallinity ratio and lead to cooperative motions. The main α relaxation has a compensation temperature close to the glass transition temperature and a compensation time around few seconds. The temperature lag between T_c and T_g is a feature of compensation effect [38]. The average value of $T_c - T_g$ is 31 K in a wide variety of crystalline polymers [28]. This compensation phenomenon is in agreement with cooperative mobility of free amorphous phase relaxation.

Vitreous response

Secondary relaxation and primary relaxation followed Arrhenius behaviour. A VTF behaviour was reported by some authors [19, 26] for the PEEK α relaxation. However, the increase of crystallinity ratio upon heating and the high chain rigidity of PEEK are responsible for this Arrhenius behaviour.

At high temperature, dielectric loss values increased and confirmed the dipolar phenomenon attributed to the rigid amorphous phase labelled α_c. Indeed, the dielectric relaxation study of poly(trimethylene terephthalate) [12] shed some on light on a strong increase in α relaxation intensity with temperature above T_g suggested a gradual mobilization of the rigid amorphous phase. The rigid amorphous phase are constrained by crystallites, the amount of free volume is restricted and leads to an higher relaxation temperature [17, 19] described by an Arrhenius law. The molecular dynamics of the dipolar entities of PolyAmide 6.9 [39] and poly(ethylene terephthalate) [40] has been analysed by DDS. The α' relaxation of PA 6.9 and the α_u relaxation of PET appeared at higher temperature than α main relaxation and were attributed to the amorphous phase constrained by crystallines lamellae. In the same manner, the influence of the amorphous confinement on the chains dynamics was probed into the fluorinated parylene (PA-F) [41] well above the glass transition temperature.

Combination of dielectric data in the whole frequency range

Comparison of DDS and TSC results allows us to correlate complex relaxations on a large frequency scale (10^{-3}–10^6 Hz). The combination of these two techniques were previously performed to studied relaxation times of Polyamide 6.9 [39], poplar cell wall [42], the poly(*n*-alkyl methacrylates) [43].

Relaxation times extracted with Havriliak–Negami equation and elementary relaxation times isolated by the fractional polarisation procedure in TSC are reported on the same Arrhenius diagram in Fig. 10. Elementary relaxation times of γ secondary relaxation and α main relaxation were matched by the τ_{HN} deduced from the Kramers–Kronig analysis. The α_c mode attributed to the rigid amorphous phase relaxation is only observed by DDS. Indeed, the temperature range studied in TSC was not enough broad to show the rigid amorphous phase phenomenon.

Table 1 Activation parameters obtained from Arrhenius fit of TSC and DDS data

	TSC		DDS	
	ΔH/kJ mol^{-1}	ΔS/J mol^{-1} K^{-1}	ΔH/kJ mol^{-1}	ΔS/J mol^{-1} K^{-1}
γ Relaxation	50	25	56	80
β Relaxation	106	34		
α Relaxation	581	100	302	485
α_c Relaxation			253	291

Activation parameters deduced from Arrhenius fitting of liquid and vitreous response are reported in Table 1.

At low temperature, the apparent activation energy is of the order of 30–45 kJ mol^{-1}, then E_a increases with temperature which is consistent with values described in literature [16, 22]. The activation parameters reflect the size of domains where cooperative mobility takes place. The low value of ΔH and ΔS pointed out localised mobility. Non cooperative γ and β relaxation involve short-chain sequences acting individually. The activation enthalpy of α relaxation confirms a cooperative delocalized mobility of nanometric sequences of the main chain. After the classical increase of ΔH with temperature, due to intramolecular interaction of electronics orbital, ΔH becomes constant, from the glass transition temperature, in a wide series of semi-crystalline polymers with semi-rigid chains [44]. Considering the influence of crystalline morphology and chain rigidity, this evolution has been assigned to the relaxation of amorphous sequences under stress from crystallites. A slight decrease of the activation parameters of PEEK, also reported by Mourgues et al. [23], is due to the establishing of local order in the rigid amorphous phase which cannot propagate cooperative movements.

The low frequency extrapolation of DDS results is in agreement with TSC results. The correlation between dielectric measurements is well suited to the analysis of dynamics continuity associated with transitions in vitreous and liquid state and to improved knowledge of PEEK molecular mobility.

Conclusions

Dielectric relaxation has been applied to thorough investigation of the dynamic molecular mobility of quenched PEEK. The combination of both dielectric spectroscopy has bringing to light the coherence between molecular

dynamics in vitreous and liquid state. At low temperature, we expect two secondary relaxation modes due to localized non-cooperative motions. The molecular origin of γ mode is due to phenyl rings oscillations, this study provides the evidence of vibration regularity between glassy and liquid phase. The β secondary relaxation mode is attributed to conformational defects. At higher temperature, the cooperativity of delocalized molecular mobility has been shown. The α relaxation of free amorphous phase occurred around the glass transition temperature. The α_c relaxation mode validated the 'three-phase model' and confirmed the existence of rigid amorphous phase constrained by crystallites. The good consistency between DDS and TSC results allows us to propose a phenomenological model explaining heterogeneity of amorphous PEEK useful in vitreous state as well as in liquid state.

References

1. Kemmish D. Update on the technology and applications of polyaryletheretherketones. Shrewsbury: ISmithers Rapra Pub.; 2010.
2. Cheng SZD, Cao MY, Wunderlich B. Glass-transition and melting behavior of poly(oxy-1,4-phenyleneoxy-1,4-phenylenecarbonyl-1,4-phenylene). Macromolecules. 1986;19(7):1868–76.
3. Sauer BB, Hsiao BS. Effect of the heterogeneous distribution of lamellar stacks on amorphous relaxations in semicrystalline polymers. Polymer. 1995;36(13):2553–8.
4. Huo PT, Cebe P. Temperature-dependent relaxation of the crystal amorphous interphase in poly(ether ether ketone). Macromolecules. 1992;25(2):902–9.
5. Arous M, Ben Arnor I, Kallel A, Fakhfakh Z, Perrier G. Crystallinity and dielectric relaxations in semi-crystalline poly(ether ether ketone). J Phys Chem Solids. 2007;68(7):1405–14.
6. Jonas A, Legras R. Relation between peek semicrystalline morphology and its subglass relaxations and glass-transition. Macromolecules. 1993;26(4):813–24.
7. Blundell DJ, Osborn BN. The morphology of poly(aryl-ether-ether-ketone). Polymer. 1983;24(8):953–8.
8. Verma R, Marand H, Hsiao B. Morphological changes during secondary crystallization and subsequent melting in poly(ether ether ketone) as studied by real time small angle X-ray scattering. Macromolecules. 1996;29(24):7767–75.
9. Ko TY, Woo EM. Changes and distribution of lamellae in the spherulites of poly(ether ether ketone) upon stepwise crystallization. Polymer. 1996;37(7):1167–75.
10. Cebe P, Hong SD. Crystallization behavior of poly(etheretherketone). Polymer. 1986;27(8):1183–92.
11. Chen H, Cebe P. Investigation of the rigid amorphous fraction in nylon-6. J Therm Anal Calorim. 2007;89(2):417–25.
12. Kalakkunnath S, Kalika DS. Dynamic mechanical and dielectric relaxation characteristics of poly(trimethylene terephthalate). Polymer. 2006;47(20):7085–94.
13. Sasuga T, Hagiwara M. Molecular motions of non-crystalline poly(aryl ether–ether-ketone) peek and influence of electron-beam irradiation. Polymer. 1985;26(4):501–5.
14. David L, Girard C, Dolmazon R, Albrand M, Etienne S. Molecular mobility in para-substituted polyaryls. 3. Low-temperature dynamics. Macromolecules. 1996;29(26):8343–8.
15. Bas C, Fugier M, Alberola ND. Reinforcement effect and molecular motions in semicrystalline peek films: mechanical and physical modelings. 1. J Appl Polym Sci. 1997;64(6):1041–52.
16. David L, Etienne S. Molecular mobility in para-substituted polyaryls. 1. Sub-t(g) relaxation phenomena in poly(aryl ether ether ketone). Macromolecules. 1992;25(17):4302–8.
17. Krishnaswamy RK, Kalika DS. Dynamic-mechanical relaxation properties of poly(ether ether ketone). Polymer. 1994;35(6):1157–65.
18. Kalika DS, Krishnaswamy RK. Influence of crystallinity on the dielectric-relaxation behavior of poly(ether ether ketone). Macromolecules. 1993;26(16):4252–61.
19. Nogales A, Ezquerra TA, Batallan F, Frick B, Lopez-Cabarcos E, Balta-Calleja FJ. Restricted dynamics in poly(ether ether ketone) as revealed by incoherent quasielastic neutron scattering and broad-band dielectric spectroscopy. Macromolecules. 1999;32(7):2301–8.
20. Verot S, Battesti P, Perrier G. Semi-empirical calculations and dielectric spectrometry of molecular units in peek. Polymer. 1999;40(10):2605–17.
21. Sakamoto WK. Dielectric spectroscopy and thermally stimulated discharge current in peek film. Eclet Quim. 2003;28(2):49–53.
22. Sauer BB, Avakian P, Starkweather HW, Hsiao BS. Thermally stimulated current and dielectric studies of poly(aryl ether ketone ketone). Macromolecules. 1990;23(24):5119–26.
23. Mourguesmartin M, Bernes A, Lacabanne C. Thermally stimulated current study of the microstructure of peek. J Therm Anal. 1993;40(2):697–703.
24. Kim EJ, Ohki Y. Ionic behavior of dc conduction in polyetheretherketone. IEEE Trans Dielectr Electr Insul. 1995;2(1):74–83.
25. Bacharan C, Dessaux C, Bernes A, Lacabanne C. Thermally stimulated current spectroscopy of amorphous and semi-crystalline polymers. J Therm Anal Calorim. 1999;56(3):969–82.
26. Goodwin AA, Hay JN. Dielectric and dynamic mechanical relaxation studies on poly(aryl ether ketone)s. J Polym Sci Pt B-Polym Phys. 1998;36(5):851–9.
27. Fougnies C, Dosiere M, Koch MHJ, Roovers J. Morphological study and melting behavior of narrow molecular weight fractions of poly(aryl ether ether ketone) (peek) annealed from the glassy state. Macromolecules. 1998;31(18):6266–74.
28. Teyssedre G, Mezghani S, Bernes A, Lacabanne C. Thermally stimulated currents of polymers. In: Runt JP, Fitzgerald JJ, editors. Dielectric spectroscopy of polymeric materials—fundamental and applications. Washington, DC: American Chemical Society 1997. p. 227.
29. Teyssedre G, Demont P, Lacabanne C. Analysis of the experimental distribution of relaxation times around the liquid-glass transition of poly(vinylidene fluoride). J Appl Phys. 1996;79(12):9258–67.
30. Delbreilh L, Negahban M, Benzohra M, Lacabanne C, Saiter JM. Glass transition investigated by a combined protocol using thermostimulated depolarization currents and differential scanning calorimetry. J Therm Anal Calorim. 2009;96(3):865–71.
31. Starkweather HW. Simple and complex relaxations. Macromolecules. 1981;14(5):1277–81.
32. Kremer F, Schönhals A. Broadband dielectric spectroscopy. Berlin: Springer; 2002.
33. Havriliak S, Negami S. A complex plane analysis of α-dispersions in some polymers systems. J Polym Sci. 1966;14:99–117.
34. Steeman PAM, vanTurnhout J. A numerical kramers-kronig transform for the calculation of dielectric relaxation losses free from ohmic conduction losses. Colloid Polym Sci. 1997;275(2):106–15.
35. Schlosser E, Schonhals A, Carius HE, Goering H. Evaluation method of temperature-dependent relaxation behavior of polymers. Macromolecules. 1993;26(22):6027–32.

36. Chen CL, Lee CL, Chen HL, Shih JH. Molecular-dynamics simulation of a phenylene polymer. 3. Peek. Macromolecules. 1994;27(26):7872–6.
37. Poliks MD, Schaefer J. Characterization of the chain dynamics of PEEK by CPMAS ^{13}C NMR. Macromolecules. 1990;23(14): 3426–31.
38. Hoffman JD, Williams G, Passaglia E. Analysis of the α, β and γ relaxations in polychlorotrifluoroethylene and polyethylene: dielectric and mechanical properties. J Polym Sci. 1966;14: 173–235.
39. Capsal J-F, Dantras E, Dandurand J, Lacabanne C. Dielectric relaxations and ferroelectric behaviour of even-odd polyamide PA 6,9. Polymer. 2010;51(20):4606–10.
40. Carsalade E, Bernes A, Lacabanne C, Perraud S, Lafourcade M, Savignac M. Transitions/relaxations in polyester adhesive/pet system. J Therm Anal Calorim. 2010;101(3):849–57.
41. Diaham S, Bechara M, Locatelli ML, Lebey T. Influence of crystallization-induced amorphous phase confinement on alpha- and beta-relaxation molecular mobility in parylene f. J Appl Phys. 2011;110(6):063703.
42. Jafarpour G, Dantras E, Boudet A, Lacabanne C. Molecular mobility of poplar cell wall polymers studied by dielectric techniques. J Non-Cryst Solids. 2008;354(27):3207–14.
43. Dudognon E, Bernes A, Lacabanne C. Nature of molecular mobility through the glass transition in poly(*n*-alkyl methacrylates): a study by dielectric spectroscopies. J Macromol Sci-Phys. 2004;B43(3):591–604.
44. Lacabanne C, Lamure A, Teyssedre G, Bernes A, Mourgues M. Study of cooperative relaxation modes in complex-systems by thermally stimulated current spectroscopy. J Non-Cryst Solids. 1994;172:884–90.